Journal of Engineering Science 11(1), 2020, 113-122

JES

an international Journal

AN EXPERIMENTAL INVESTIGATION OF RELATIONSHIP BETWEEN SURFACE HARDNESS AND STRENGTH OF LOCALLY PRODUCED TMT 500W BAR IN BANGLADESH

Sazzad Ahmad[1] and Wahidur Rahman Sajal[2]

[1]*Department of Materials Science & Engineering, Chittagong University of Engineering & Technology, Chattogram-4349, Bangladesh*

[2]*Department of Materials Science and Engineering, Khulna University of Engineering & Technology, Khulna-9203, Bangladesh*

Received: 11 April 2020 Accepted: 30 May 2020

ABSTRACT

The high-strength mild steel bars (usually low carbon steel) are widely used for structural purposes throughout the world including Bangladesh. The strength of these deformed barsis measured through a sample decimation process via Universal Testing Machine (UTM), after which the broken pieces are discarded as scrap for recycling. Therefore, measuring the hardness of steel could be a good indication of strength and will involve less sample and short time for testing. The strength–hardness relationship for steel and cast iron is well defined. However, the TMT 500W deformed bar using in Bangladesh has different structural phenomena due to its unique fabrication technique. Therefore, it is necessary to understand how the strength varies with hardness for this grade of steel. The current research aims to explore the hardness–strength relationship for TMT (Thermo-mechanical Treatment) 500W bar as an alternate of the tensile test to minimize the wastage, cost and time of testing. Several TMT 500W bars were collected from the local market and measured the Rockwell Hardness B (HRB), strength and other relevant macroscopic/microscopic parameters. Finally, two empirical relationships of yield and tensile strength have been established using rim hardness, core hardness, and rim thickness data. The actual strength data shows a good agreement with present findings and the result variation is found less than 2% and 3% in the case of yield strength and tensile strength respectively.

Keywords: *Deformed Bar; Microscope; Core; Rim; Rockwell Hardness; TMT Bar.*

1. INTRODUCTION

Structural steel has a significant impact on today's civilization and most widely used than any other material. From the beginning of its first discovery still, it is serving quietly to the society by the virtue of its easy formability, good strength and superior fracture toughness. Undoubtedly, the most significant breakthrough for steel construction in the last century came with the advent of welding as the primary technology for joining. The primary function of structural steel is to reinforce the concrete structure by allowing slight bending stress and prevent the fracture during tensile load conditions. The high-rise skyscraper that we are being built today has made possible by blessings of this structural steel. For diverse properties, structural steel is nowadays also used for constructing high rise buildings structure, steel bridges, offshore steel platforms and so on. For all the above-mentioned applications, the most frequent useable property of steel is yield strength and beyond this strength, the structure will deform permanently. Therefore, the structural steel is widely specified according to its yield strength e.g. 60 Grade (*i.e.* 60 kpsi yield strength), 500W (*i.e.* 500 MPa yield strength), etc.

High strength steel is highly demanded by the structure design engineer for reducing the overall weight of the building structure and that will provide more safety against earthquakes. The strength of the steel can be enhanced by various means e.g. adjusting the chemical composition (Grade steel, micro-alloyed steel), induced plasticity by cold twisted and deformed (TOR steel), refining the grain size (UFG steel), adjusting the hard and soft phase of the structure (dual-phase steel), quench and subsequent tempering (TMT/QT steel) and adjusting metastable phase proportion (TRIP steel).

History of structural steel development in Bangladesh is started with adjustment of chemical composition during production. In that case, the relative composition is increased with the size of the steel bar and that is detrimental for its bendability and weldability property. The recent introduction of QT (quenched and temper) bar has successfully overcome those shortcomings of the chemical enhanced deformed bar. Many companies in Bangladesh also has branded the QT bar as TMT (thermo-mechanical treatment) bar. Apart from chemical composition, the basic difference of these two products lies in the final stage of cooling where the TMT bar undergoes a forced cooling by passing through a water bath and the chemically treated bar is cooled naturally in the air. Figure 1 shows the basic microstructural feature of a TMT bar after etched in a 2% Nital solution.

* Corresponding Author: sazzad@cuet.ac.bd

ISSN 2075-4914 (print); ISSN 2706-6835 (online)

Whereas, the microstructural feature of a typical 40/60 grade steel shows only a similar microstructure at zone–3 as shown in Figure 1 *i.e.* mixture of ferrite and pearlitic structure only (Bleck *et al.*, 2004). Remarkably, the soft–core and hard–case type composite structural feature gives the TMT bar extra bendability and elongation than Grade–60 steel. The basic comparison of these two steel is shown in Table 1.

The common quality factor of reinforced steel bar includes the right chemical composition, proper yield, and ultimate strength, minimum elongation up to fracture, and crack resistance during bend test. Among them, the yield strength of the reinforced steel bar is the point of interest of the user and the manufacturer both. Knowing the proper yield strength of steel reduces the chances of permanent failure of the structure. Most commonly, the TMT bar producers usually use a Universal Tensile Machine (UTM) for routine quality checking purposes where a significant number of discard bar produces after every tensile test. Therefore, measuring the hardness of steel could be a good indication of strength and will involve less sample and short time for testing.

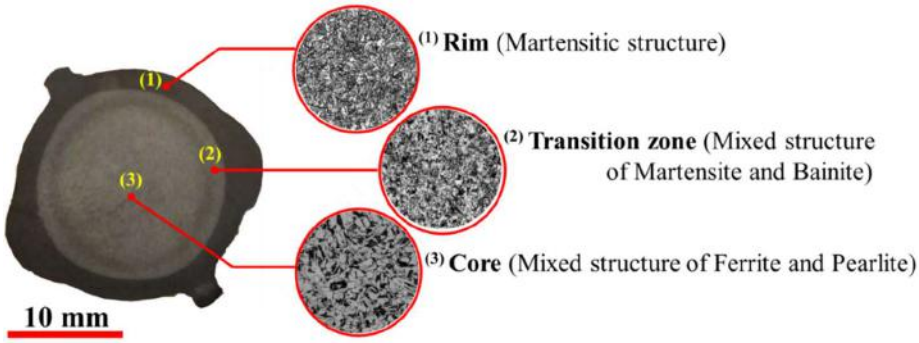

Figure 1: Microstructural features of a TMT bar after 2% Nital etching (adopted from Capitol Steel, 2020)

Table 1: Comparison of TMT 500W and Conventional Grade-60 Deformed Bar (Arefin, 2019)

Type	Yield Strength (MPa)	%C	%Si	%Mn	%S	%P	Others
Plain Carbon TMT 500W Bar	500 min	0.25 max	0.25-0.30	0.70-1.20	0.05 max	0.05 max	Trace
Typical Grade-60 Bar	420 min	0.25-0.38	0.30-0.50	0.70-1.50	0.05 max	0.05 max	Trace

The hardness of metal represents the resistance of localized plastic deformation during indentation. It is a quick method of determination of materials property without mass loss of materials. Moreover, several investigations were carried out to correlate those two properties *i.e.* Hardness and materials strength (Pavlina and Van Tyne, 2008; Busby *et al.*, 2005; Ray *et al.*, 1997; Cahoon *et al.*, 1971). The study of hardness–strength relationships will be helpful where the direct measurement of tensile properties of a material is not possible due to smaller in size or complex shape. In another way, knowing the strength value from hardness data will greatly reduce the test sample volume which will save money and time.

Many empirical relationships of hardness and strength are available in the literature and one of such relations (Tabor, 2000; Ashby and Jones, 1980) is:

$$H = 3\sigma_y \quad (1)$$

Where H= Hardness and σ_y = yield strength of a perfectly plastic material which is not work-harden. Tabor (2000) proposed that the yield strength should be compensated by the uniaxial flow stress at a given strain value for work-hardening metals *e.g.* for a Vickers indenter, the typical strain is between 8% and 10%, and the hardness at this strain value is then 3 times the flow stress. In another way, indentation could induce work-hardening behavior, and only one-third of the hardness value represents strength after hardening.

However, the relationship between ultimate tensile strength (UTS) and hardness is also stated in several publications besides the yield strength (Callister and Rethwisch, 2007; Boyer and Gall, 1985).

$$H_v \approx 3\sigma_{UTS} \quad (2)$$

Where H_v = Vickers hardness number and σ_{UTS}= Ultimate Tensile Strength of the materials.

Therefore, as per equation (1) and (2) another question arises: does one-third of the hardness reflect the yield strength or the ultimate tensile strength of the materials? Later on, Cahoon (1972) provided hardness *vs* yield strength and tensile strength expression in the form of:

$$\sigma_y = \frac{H}{3}(0.1)^n \quad (3)$$

$$\sigma_{UTS} = \frac{H}{2.9}\left(\frac{n}{0.217}\right)^n \quad (4)$$

Where ***n*** is the strain hardening exponent and can be measured directly from the uniaxial tensile test or indirectly from Meyer's hardness.

All the above discussions are related to the uniform structured material however as it has been shown earlier in Figure 1 that the TMT bar consists of dissimilar microstructure *i.e.* rim, transition layer, and core region thereforethe strength vs hardness relationship may not be straight forward like uniform structured materials. Dani and Palit (2015) showed an empirical relation based on the rim and core hardness (VHN) plus martensitic rim thickness is as follows:

$$Yield\ strength = \frac{(K_1 \times Rim\ Hardnes + K_2 \times Core\ Hardness + K_3 \times Martensitic\ rim\ thickness)}{3} \quad (5)$$

Where, K_1, K_2, and K_3 are proportional constants, derived from the ratio of strength *vs* rim hardness, core hardness, and martensitic rim thickness. Dani and Palit (2015) assumed that the yield strength of the TMT bar is linearly varied with rim hardness, core hardness, and martensitic rim thicknessand their calculated value for K_1, K_2, and K_3 are 2.13, 3.35 and 203.03, respectively.

Karunaratne *et al.* (2014) showed that the 0.1% proof stress (stress similar to yield strength, used when yield strength cannot measure directly) of TMT bar increases with martensitic rim thickness increases however, they did not represent any formula for this relationship. Kabir (2014) used another experimental relationship of hardness and strength similar to the law of mixture for composite materials as per the following equation:

$$Strength = \%Case\ area \times Case\ strength + \%Core\ area \times Core\ strength \quad (6)$$

Where a standard chart for hardness to strength conversion (ASTM A370-68) was used to calculate the case and core strength of equation (6).

To further improvethe understanding of how strength varies with hardness of rim, transition zone, and core regionwe examine the strength, hardness, macro, and microstructure of commercially available TMT 500W bar and tries to set up a correlation of strength andhardness of different position of the TMT bar. This technique will enable to determine in–situ strength evaluation during production in industriesto reduce the sampling size for testingand also be useful to simulate the physical property during thermo-mechanical treatment or heat-treatment process.

2. EXPERIMENTAL METHODOLOGY

In the current study, a systemic approach was followed where the work involved to sample preparation, hardness test, tensile test execution, data collection, and result analysis. The description of the sample preparation process and different measurement techniques are discussed in the following section including tensile test, hardness test, and chemical composition analysis processes.

2.1 Experimental Samples

Locally produced 7 pieces of 500W TMT high-strength steel bars of 20 mm diameter were used in this experiment. Each sample was 600 mm long and later on, different sub–sample was prepared from the initial long sample for further investigation.

2.2 Tensile Test

For the tensile test experiment, a 500-mm long sample was taken from the initial sample. The test was conducted using a digital UTM (Model: TUE-C-400) and followed BDS-ISO:6935-2 standard. Initially, the sample was marked to 5D gauge length (*D*= diameter of the bar) on the longitudinal surface for elongation measurement and then weighted in a digital balance to measure the mass per unit length. Afterward, the sample was griped between the two jaws and tare the initial load and elongation data of the machine. The load was maintained at a constant rate, 0.4 min^{-1} (±20%) until the fracture of the sample occurred. A digital stress-strain curve and relevant information obtained from the WinUTM software. Finally, the broken sample was removed from the setup and calculates the elongation measurement manually.

2.3 Microscopic and Macroscopic Analysis

An attempt was made to observe the microscopic features: rim, transition, and core region's structures and macroscopic features: the rim thickness of each sample. Initially, a 25 mm (approx.) long sample was taken from each of the main sample bars and cold-mounted using epoxy resin and hardener of 2:1 ratio in a mold. After 8 hours, the samples were released from the mold and used for further polishing. In the beginning, the samples were polished against a 120 grit, SiC emery paper and later on 240, 320, 400, 600, 800, 1000, 1200, and 1500 grit paper successively. Figure 2 shows the epoxy mounted, cold-set samples after coarse polished in 120 to 1500 grit emery papers. Afterward, fine polishing was carried out in a semi auto-polishing machine using 1 µm gamma-alumina paste. The final samples were etched by 2% Nital solution and analyzed the macroscopic and microscopic features using a digital metallurgical microscope (Model: Amscope ME520TA). Furthermore, the same samples were used for hardness analysis.

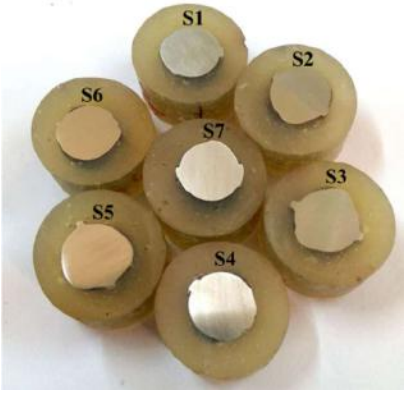

Figure 2: Cold mounted samples after coarse polishing

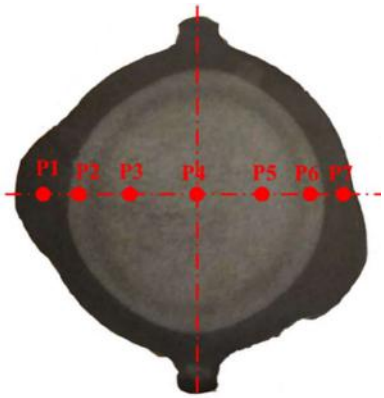

Figure 3: Hardness measurement location identification.

2.4 Hardness Test

As mentioned earlier, the samples used for macro/microscopic analysis have been used for hardness measuring purposes. The hardness of the samples was measured using a Rockwell hardness tester (Model: MRP–1). For each sample, 7-10 different readings were taken from several positions of the sample as shown in Figure 3 where points P1 and P7 are left and right position of the rim area respectively. Similarly, P2 and P6 are the transition zone hardness and P3 and P5 are the mid-center (middle between surface and center) hardness respectively,whereas point P4 represents the core or center hardness of the bar.

2.5 Image Analysis using Image Pro

An image analysis software *viz.* Image Pro was used to calculate the percentage of rim area as compared to the total surface area. Figure 4 shows a sample calculation using Image-Pro software. For simplification of the calculation, the outer–rim area was assumed as a circle. Therefore, the inner–rim area was selected manually for asymmetric rim thickness and circular selection for homogeneous rim thickness as shown in Figure 4.

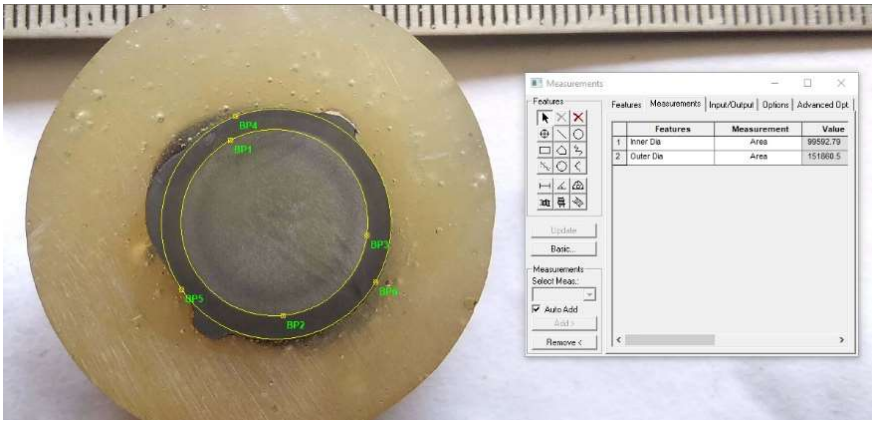

Figure 4: Calculation of percent rim area through Image pro software

Finally, the percent of rim area was calculated using the following equation:

$$\% \text{ Rim area} = \frac{\text{Outer area} - \text{inner area}}{\text{outer area}} \times 100\% \quad (7)$$

2.6 Chemical Composition Analysis

The chemical composition of the samples was determined using a Spark–OES machine (Model: Spectrolab, M10) facility availed from a local steel plant at Dhaka. A 25mm long sample piece was collected from each initial sample and used for Spark-OES analysis. The samples were polished to one side in a 60-grit emery paper for flattening the analyzing surface and then set to the OES machine. Three consecutive sparks were taken for each sample and took the average value.

3. RESULTS AND DISCUSSION

The experimental results obtained from different tests and their analyses are discussed in this section. The tensile and hardness test data, micro and macrostructural analysis results are presented. Later on, an attempt is made to relate these hardness and tensile test data in a correlation to other variables e.g. martensitic rim thickness, percentage of rim area and sample composition.

3.1 Chemical Composition Results

The compositional analysis data are shown in Table 2. From the compositional analysis of the deformed bars, it can be seen that all the samples have a more or less similar chemical composition. The corresponding carbon equivalent value (C.E.1 and C.E.2) of all samples vary in a limited range *i.e.* $C.E.1_{(average)}$: 0.33 (±0.02) and $C.E.2_{(average)}$: 0.37 (±0.02). This signifies the negligible effect of compositional variability on other test results.

Table 2: Chemical composition (% wt.) of the experimental samples

Elements	S1	S2	S3	S4	S5	S6	S7
C	0.21	0.21	0.23	0.23	0.23	0.22	0.22
Si	0.21	0.16	0.23	0.21	0.22	0.22	0.20
Mn	0.70	0.54	0.51	0.74	0.74	0.73	0.54
P ($\times 10^2$)	0.30	0.40	1.30	0.10	0.20	0.50	1.00
S ($\times 10^2$)	1.50	0.10	2.10	0.40	1.30	1.00	0.40
Cr	0.07	0.11	0.09	0.05	0.05	0.12	0.11
Mo	0.02	0.01	0.01	0.01	0.01	0.01	0.01
Ni	0.06	0.06	0.06	0.04	0.05	0.06	0.06
Al ($\times 10^2$)	0.20	0.40	0.40	0.20	0.30	0.30	0.30
Cu	0.13	0.14	0.15	0.14	0.14	0.23	0.17
Nb ($\times 10^3$)	0.50	0.90	1.40	0.50	0.30	0.20	0.50
Pb ($\times 10^3$)	0.20	0.20	0.40	0.20	0.20	0.20	0.30
Sn ($\times 10^2$)	1.00	1.50	3.40	1.10	0.70	0.90	2.10
Sb ($\times 10^3$)	0.40	0.50	1.10	0.40	0.40	0.40	1.80
Fe	98.6	98.7	98.6	98.6	98.5	98.4	98.7
C.E.1	0.33	0.30	0.32	0.35	0.35	0.35	0.31
C.E.2	0.36	0.34	0.35	0.38	0.37	0.39	0.35

Carbon Equivalent: (i) $C.E.1 = C + \frac{Mn}{6}$; (ii) $C.E.2 = C + \frac{Mn}{6} + \frac{Cr + Mo + V}{5} + \frac{Cu + Ni}{15}$

Table 3: The tensile test and unit weight data of the test bars

Properties	S1	S2	S3	S4	S5	S6	S7
Yield Strength (MPa)	526	529	550	550	520	532	500
Tensile Strength (MPa)	630	640	665	658	613	635	602
T/Y Ratio	1.20	1.23	1.21	1.20	1.18	1.19	1.20
Elongation (%)	20	21	19	21	21	18	23
Unit Weight (Kg/m)	1.571	1.565	1.573	1.570	1.564	1.578	1.553

3.2 Tensile Test Results

All the seven samples (S1 to S7) were tested and the tensile test data obtained from the UTM machine is shown in Table 3. All the test samples have yield strength of ≥500 MPa. The ratio of tensile to yield strength (T/Y ratio) of the test samples lies on average 1.20 (±0.01) which will help to derive one strength from others when

only one value is possible to determine. The elongation of all the deformed bars showed significant deformation after fracture and average elongation is 21% at 5D (*D*= Diameter, 20 mm) gauge length.

Figure 5 shows the fractured sample after the tensile test. It appears that there is a reduction of area at fracture zone which signifies the ductile behavior the bars. Moreover, the fractography of the samples shows a cleavage type fracture, initiated from the sample's surface and propagate along a transverse-rib direction *i.e.* 45^{o} shear.

3.3 Macroscopic and Microscopic Analysis Result

Each of the samples was etched in 2%-Nital for 5 to 7 seconds to reveal the macroscopic and microscopic images. Figure 6 shows the macroscopic features of all seven samples. It can be seen from Figure 6 that there is a variation of martensitic rim thickness (dark black color in the images) among the samples. Samples 6, and 7 have non-uniform rim thickness and sample-7 has the lowest rim area. Table 4 shows the fraction of the rim area of the samples and it is revealed that the percent of the rim area for sample-7 is only 18% and the tensile test data are also consistent with this finding. The experimental observation ofDani and Palit (2015) and Karunaratne *et al.* (2014) also confirm that the strength reduces when rim thickness/area decreases.

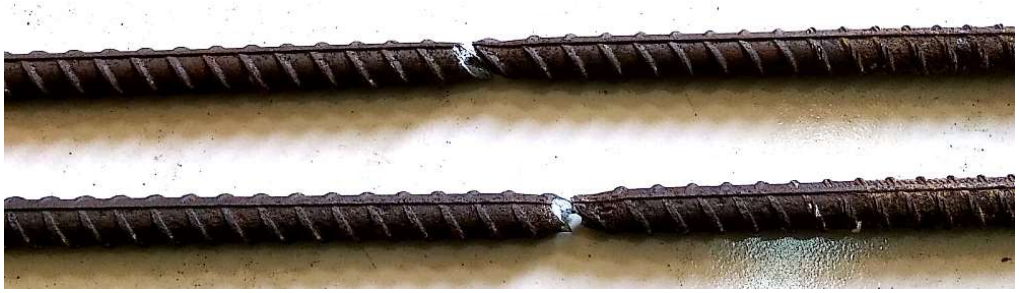

Figure 5: Fractured samples after the tensile test

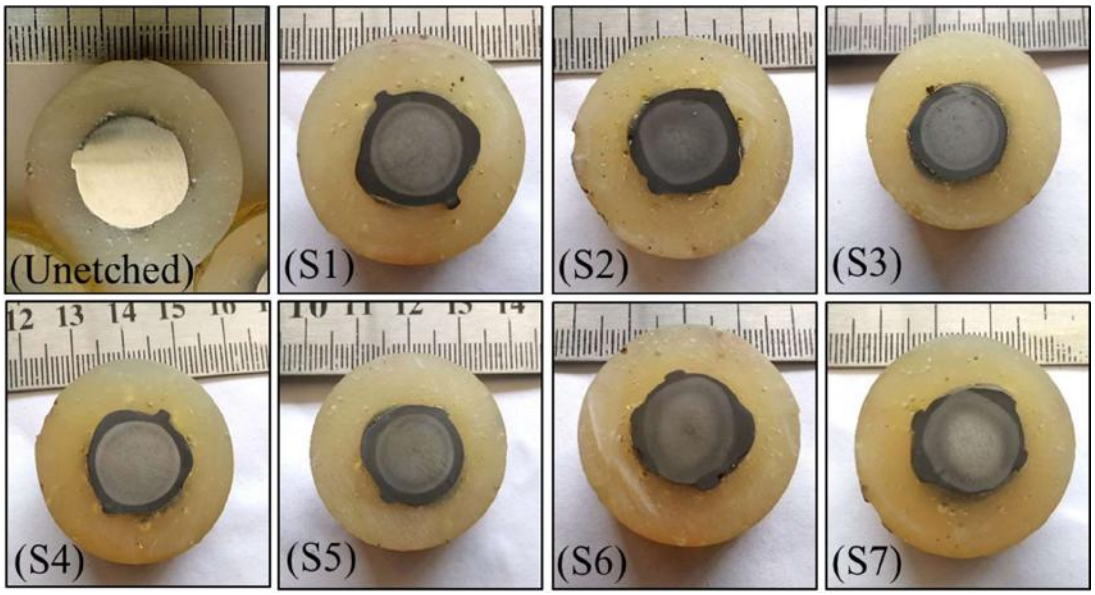

Figure 6: The macroscopic images of the samples after etched in a 2% Nital solution.

Table 4: Percent of rim area of the TMT bar estimated from image processing

	S1	S2	S3	S4	S5	S6	S7
Rim Area (%)	32.2	32.1	32.5	31.9	34.4	25.2	18.2

The microstructural features of the TMT bar are shown in Figure 7 where the core and rim structures are illustrated only. As the samples consist of plain carbon steel's composition (Table 2) therefore at the core (center) region the microstructure consists of hypoeutectoid (ferrite+pearlite) structure. As the surface of the TMT bar is quenched during production therefore the surface of the bar (*i.e.* rim) is consisted of acicular (needle-like) martensitic structure. The transition zone microstructure contains bainite structure (Dani and Palit, 2015) as similar to diffuse microstructure of martensitic structure, which is not shown here.

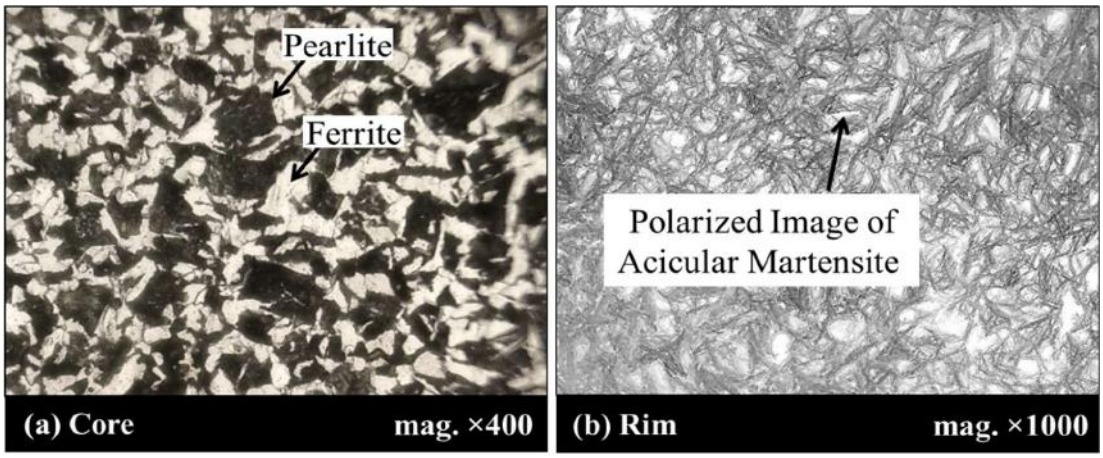

Figure 7: Microstructural images of the core and rim region of an etched bar.

3.4 Hardness Results

It has been shown in the previous section that the TMT bar consists of dissimilar microstructure at different zone therefore it is quite expected that the sample will have different hardness values at different zone. We know, martensite is a metastable phase of BCT (Body-Centered Tetragonal) structure which is created as a result of lattice distortion of BCC structure due to incomplete carbon diffuse-out process during quenching (Avner, 1974). As martensite is the most unstable phase of a TMT bar therefore, it shows the highest hardness as compared to ferrite and pearlite. Initially, the hardness of a TMT bar was measured through a line of the cross-section as shown in Figure 8(a). The hardness measurement point details have been shown in Figure 3.

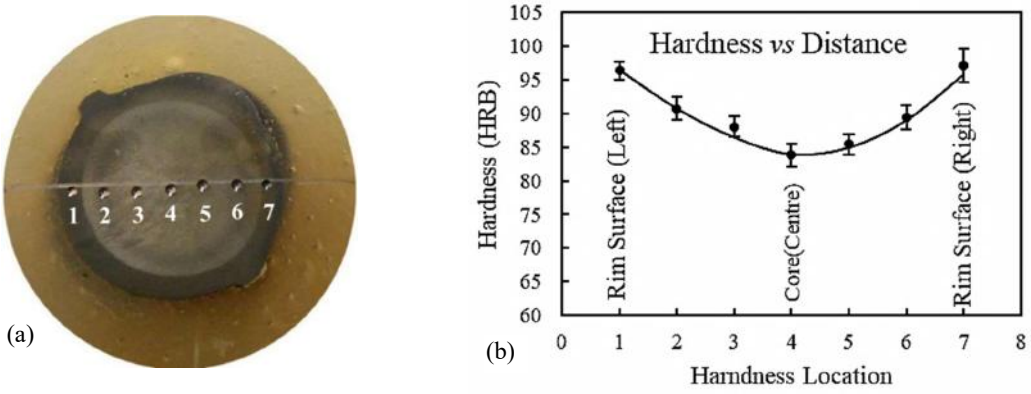

Figure 8: Hardness measurement (a) Different hardness measured position of the mounted sample S1 (b) Hardness variation at different location of the sample's surface

The plot of the hardness value against the position is shown in Figure 8(b). The figure illustrates that the hardness is gradually decreasing from the surface to the core and follow a U-shaped pattern. The surface (point 1 and 7) has the highest hardness due to martensitic structure and the core (point 4) has the lowest hardness for ferrite and pearlite structure. To check the reproducibility of the data, several measurements were carried out for each position of a sample. Figure 9 shows the hardness deviation data for four-different regions *viz.* (a) rim (b) transition zone (c) mid-center (d) core.

It can be seen from the above figure that there is a slight variation of hardness value for the same position of different samples. This is due to the different proportions of the rim, transition zone, and core microstructure through the cross-section which arise due to different cooling rates during the quenching process. Hardness at core position (point 4) shows relatively a higher deviation as compared to the other region.

3.5 Hardness and Strength Relationship

Hardness and strength data obtained from their respective tests are tried to correlate using different equation exist in the literature. Initially, a linear regression type relationship was attempted to establish and a sample calculation of rim hardness *vs* yield/tensile strength plot is shown in Figure 10. It can be seen from the figure

that the curve fitting value (R^2) is good enough for the yield strength but relatively less fitted for tensile strength data.

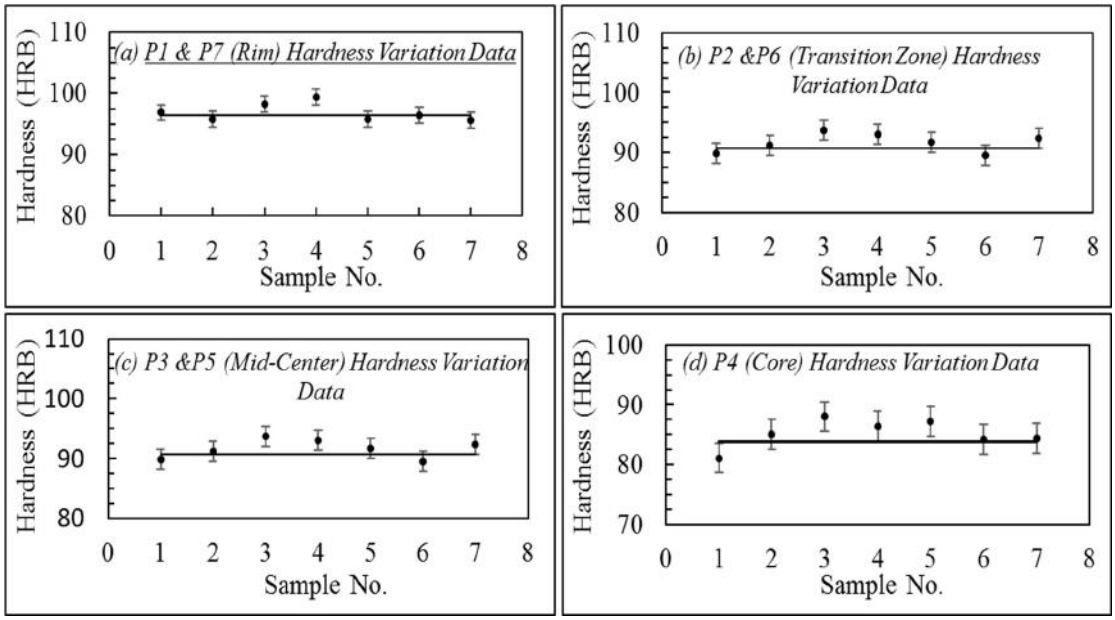

Figure 9: Hardness variation data at different position of the sample

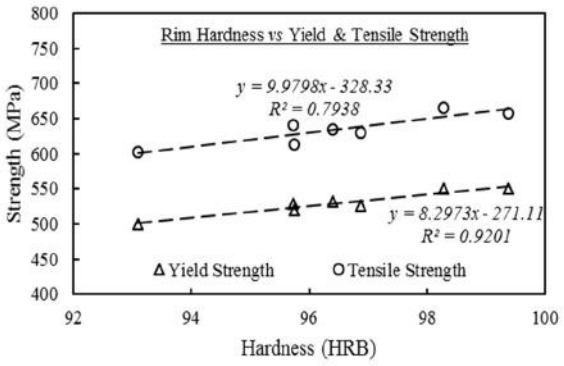

Figure 10: Rim hardness vs Strength relationship in a linear regression plot.

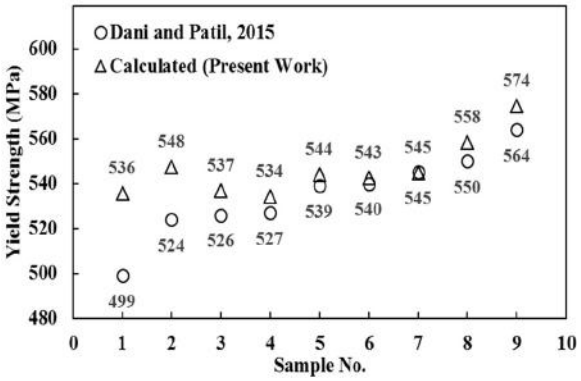

Figure 11: A Comparison of experimental and calculated tensile strength

A summary of the linear regression relationship of the hardness of different position *vs* strength is given in Table 5. It is revealed that the curve fitting data for different hardness positions is very low except for the rim hardness. It might be due to the mixture of different phases at different location *e.g.* at transition zone: (ferrite+bainite) mixture, mid-center: fine (ferrite+pearlite) mixture and core: coarse (ferrite+ pearlite) mixture.

Table 5: Linear regression relationship of strength *vs* hardness of different position

Hardness	Yield Strength		Tensile Strength	
Position	Equation	R^2	Equation	R^2
Rim	$S_{yield} = 8.2973\ H_{rim} - 271.11$	0.92	$S_{tensile} = 9.9798\ H_{rim} - 328.33$	0.79
Transition	$S_{yield} = 5.0757\ H_{trans.} + 169.77$	0.13	$S_{tensile} = 3.3907\ H_{trans.} + 218.98$	0.10
Mid-center	$S_{yield} = 6.1835\ H_{mid.c} + 83.526$	0.16	$S_{tensile} = 4.1245\ H_{mid.c} + 161.92$	0.12
Core	$S_{yield} = 5.985\ H_{core} + 16.739$	0.28	$S_{tensile} = 6.7188\ H_{core} + 59.005$	0.21

**H= Hardness; S= Strength*

It is also clear from the above data chart that the hardness vs strength relationship for transition zone and mid-center are the least fitted and the rim and core are the two most fitted plots. Moreover, the microstructure of the

latter two regions has less diversity as compared to the others since the former two areas are difficult to calculate from image analysis due to progressive etching color change e.g. Figure 6. Therefore, a combination of equations from Table 5 of rim and core hardness and relative volume-fraction of these two regions (Table 4) are used to establish a lever rule type (Callister and Rethwisch, 2007), strength-hardness relationship as follows:

$$Yield\ Strength = (1 - Fraction\ Rim\ area) \times (8.2973 H_{Rim} - 271.11) + Fraction\ Rim\ area \times (5.985 H_{Core} + 16.739) \quad (8)$$

Similarly, for tensile strength the combined equation is as follows:

$$Tensile\ Strength = (1 - Fraction\ Rim\ area) \times (9.9798\ H\_Rim - 328.33) + Fraction\ Rim\ area \times (6.7188\ H\_core + 59.005) \quad (9)$$

An attempt was made to calculate the yield strength of the samples which were used in this study by using equation (8) and the result represents in a tabular form as shown in Table 6.

It can be seen from the above data chart that the established relationship for yield strength and hardness is fitted well and the percent deviation of actual and calculated yield strength is very low (<2%). Similarly, the tensile strength of the TMT bar was calculated using equation (9) and the data are as shown in Table 7.

Table 6: Calculation of yield strength using pre-set equation (8)

Sample ID	Rim Hardness (HRB)	Core Hardness (HRB)	Yield Strength (MPa)	Rim Area (%)	Yield Strength (Calculated) Eq. (8)	Deviation (%)
S1	96.9	84.4	526	32.2	529	0.6
S2	95.7	85.1	529	22.2	524	-1.0
S3	98.3	88.0	550	32.5	544	-1.1
S4	99.4	86.4	550	34.4	547	-0.6
S5	95.7	87.3	520	31.9	528	1.6
S6	96.4	84.2	532	25.2	527	-1.0
S7	93.1	84.4	500	18.2	505	1.0

Table 7: Calculation of tensile strength using the formulated equation for this experiment

Sample ID	Rim Hardness (HRB)	Core Hardness (HRB)	Tensile Strength (MPa)	Rim Area (%)	Tensile Strength (Calculated) Eq. (9)	Deviation (%)
S1	96.9	84.4	630	32.2	634	-0.7
S2	95.7	85.1	640	22.2	628	1.9
S3	98.3	88.0	665	32.5	652	2.0
S4	99.4	86.4	658	34.4	655	0.4
S5	95.7	87.3	613	31.9	633	-3.3
S6	96.4	84.2	635	25.2	631	0.6
S7	93.1	84.4	602	18.2	605	-0.6

From the above Table 7, it is evident that the formulated tensile strength equation from hardness data is worked well andthe percent deviation of the actual and calculated value of tensile strength is < 3%. All the calculated values are close to their actual tensile strength except for sample 5 which might be due to experimental error. An attempt was made to check the feasibility of yield strength equation (8) by using data of Dani and Palit (2015) and the result is shown graphically in Figure 11.

It can be seen from Figure 11 that the present work is fitted well with the study of Dani and Palit (2015) except the slight variation in a few data. There are few reasonsbehind these differences *e.g.* the difference in sample diameter, hardness measuring scale, and rim thickness data. Dani and Palit (2015) used 25 mm diameter samples for their study whereas it is a 20 mm diameter in present work. For hardness measurement, they used the Vickers Hardness technique (HV/10Kgf) which was further converted to HRB scale using standard hardness conversion chart (ASTM Standard Hardness Conversion Tables) to fit the current study. Moreover, the rim thickness data from their work wasconvertedto the rim area by considering the standard nominal area which may lead the differences in calculation while comparing these two works.

4. CONCLUSION

Most generally, manufacturers of the TMT bar typically follow a tensile test for routine quality control purposes where a significant number of discard bars are generated after each traction test. By knowing the strength value from its hardness data will significantly reduce the volume of the test sample which will save both money and time. The goal of the current study is to investigate the hardness-strength relationship of the commercially available TMT 500W deformedbar in order to enable this technique to evaluate in-situ strength assessment during industrial production. In this work we examined the strength, hardness, macro, and microstructure of TMT bar and try to set up a correlation of strength and hardness of different position of the TMT bar. It has been observed that the strength of a TMT bar is not directly related to any particular hardness value of any specific region, rather than it relates to a combination of rim hardness, core hardness, and martensitic rim area. Therefore, two empirical relationships have been established for yield and tensile strength using linear regression relationship of strength vs hardness plus the percentage of rim-area data. The calculated strength value using established relationships shows a good fitting with experimental value with a deviation of <2% and < 3% in case of yield strength and tensile strength respectively. The research findings would be useful to reduce the sampling size for testingand also to simulate the physical property during thermo-mechanical treatment or heat-treatment process.

ACKNOWLEDGMENT

The author would like to thanks University Grant Commission (UGC) for providing the financial support to this research project through Committee for Advanced Studies and Research (CASR), KUET.

REFERENCES

Arefin, S., 2019. Rahim Steel Mills Ltd., Internal Quality Control Report, Unpublished.

Ashby, M., and Jones D., 1980. Engineering Materials I, Pergamon Press, Oxford, pp 105.

Avner, S. H., 1974. Introduction to Physical Metallurgy, 2nd ed., McGraw-Hill New York.

Bleck, W., Papaefthymiou S., and Frehn A., 2004. Microstructure and tensile properties in dual phase and trip steels, Steel research international, **75**(11), 704-710.

Boyer, H. E., and Gall T. L., 1985. Metals handbook; desk edition.

Busby, J. T., Hash M. C., and Was G. S., 2005. The relationship between hardness and yield stress in irradiated austenitic and ferritic steels, Journal of Nuclear Materials, **336**(2), 267-278.

Cahoon, J. R., 1972. An improved equation relating hardness to ultimate strength, Metallurgical and Materials Transactions B, **3**(11), 3040-3040.

Cahoon, J. R., Broughton W. H., and Kutzak A. R., 1971. The determination of yield strength from hardness measurements, Metallurgical and Materials Transactions B, **2**(7), 1979-1983.

Callister, W. D., and Rethwisch D. G., 2007. Materials science and engineering: an introduction, 7, John wiley & sons New York, pp 160, 261.

Dani, M. S., and Palit M. P., 2015. Correlation of Micro-Macro Properties with Mechanical Properties in Rebar, International Journal of Engineering Research & Technology (IJERT), 4(12).

http://capitolsteel.com.ph/deformed-bars-faq/. Capitol Steel, Frequently Asked Question: Structure of a Quenched & Tempered Rebar, Access on 14-May, 2020.

Kabir, I. R., 2014. Modelling of structure-property relationship of TMT high strength structural steel bars, M. Sc. Thesis, Bangladesh University of Engineering and Technology.

Karunaratne, P., Udawatta S., and Guluwita S., 2014. A Study on the Relationship between the Martensite Layer Thickness and the Yield Strength of TMT Reinforcing Bars, SAITM Research Symposium on Engineering Advancements 2014.

Pavlina, E., and Van Tyne C., 2008. Correlation of yield strength and tensile strength with hardness for steels, Journal of Materials Engineering and Performance, **17**(6), 888-893.

Ray, A., Mukerjee D., Sen S., Bhattacharya A., Dhua S., Prasad M., Banerjee N., Popli A., and Sahu A., 1997. Microstructure and properties of thermomechanically strengthened reinforcement bars: a comparative assessment of plain-carbon and low-alloy steel grades, Journal of materials engineering and performance, **6**(3), 335-343.

Tabor, D., 2000. The hardness of metals, Oxford university press,pp 102, 191, 195.